
342. Fellenius, B.H., 2014. Analysis of results from routine static loading tests with emphasis on the bidirectional test. Proceedings of the 17th Congress of the Brasiliero de Mecanica dos Solos e Egenharia, Comramseg, Goiania, Brazil, September 10 - 13, 22 p.

COBRAMSEG 2014
9 a 13 de setembro de 2014 - Goiânia/GO - Brasil
XVII Congresso Brasileiro de Mecânica dos Solos e Engenharia Geotécnica
VII Congresso Luso-Brasileiro de Geotecnia
VI Simpósio Brasileiro de Mecânica das Rochas
VI Simpósio Brasileiro de Jovens Geotécnicos

# Analysis of Results from Routine Static Loading Tests with Emphasis on the Bidirectional Test

Bengt H. Fellenius, Dr.Tech., P.Eng.
Consulting Engineer, Sidney, BC, Canada, V8 2BL. E: Bengt@Fellenius.net

**SUMMARY** Records from routine static loading tests on four full-scale piles are analyzed: a head-down test on a driven precast concrete pile, a bidirectional test on two full-displacement-piles, a combination of dynamic and head-down static tests on a continuous-flight augercast pile, and a head-down test on a jacked-in strain-gage instrumented pile. The load-movement curves are simulated in effective stress analysis by t-z and q-z functions and the importance of separating shaft and toe resistance for achieving a correct simulation result is emphasized. The advantage of a bidirectional test over the head-down test is demonstrated in numerical simulation of the measured test responses. The effect of residual load is demonstrated and methods to determine the true resistance distributions are presented. The potential complications of strain-gage measurements and their interpretations are discussed.

KEYWORDS Static bidirectional test, dynamic test, residual load, capacity, instrumentation.

## 1 INTRODUCTION

The use of the results of a static loading test is generally thought of as a straight-forward task. Many consider that the primary objective of a test is to establish the capacity of the pile and expect that, if the actual working load is adequately smaller than the capacity, the foundation is safe. However, pile capacity is a rather diffuse value. First, the methods for how capacity is determined from the results of a static loading test vary considerably, as they can be based on the shape of the pile-head load-movement curve, on a specific intersection with that curve, a pile head load for a specific pile toe movement, or, simply, on a pile-head movement as a specific percentage of the diameter of the pile. The engineering practice shows little consensus in what definition to use. Second, a loading-test may be performed under conditions not representative for the actual service conditions, such as residual load, influences due to the soil set-up, test method, and proximity to reaction piles, which might affect the test pile response to the applied loads. In the following, four actual case histories of routine tests on full-scale piles are used to demonstrate how to analyze routine static loading tests in order to obtain better background for a design decision pertaining to pile foundations.

## 2. METHODS OF TESTING

### 2.1 The Head-down Static Loading Test

The conventional way to determine the response of the pile to axial load is to perform a static loading test by applying load to the pile head and measure the ensuing pile head movement. Usually, the tests are accompanied with soil exploration records. Regrettably, most tests do not include any attempts to determine load distribution or pile toe movement. Even with this minimum of records, such tests still provide information useful for the design of piled foundations at the specific site. A case-history paper by Meyerhof et al. (1981) is a representative example. The authors presented results of static loading tests on two test piles Type Herkules H420 and H800, which are 220 and 305 mm diameter, hexagonal shape, precast concrete piles, usually assumed to have a 30 GPa E-modulus. The piles were driven to 12 and 13 m depth, respectively, in a compact to dense overconsolidated glacial clay till at the Stewiacki River, Nova Scotia, Canada. The site investigation included a conventional borehole and two screwplate tests. At the time, these piles were usually assigned working loads of 600 and 900 kN, respectively.

Figures 1A and 1B show the distribution of water content, Atterberg limits, and undrained shear strength, and STP N-indices at the test site. The water content, about 10 %, corresponds to a 2,250-kg/m$^3$ total density and a 0.32 void ratio. The N-index bars indicate that the till was compact to 7 m depth and dense to very dense below that depth. The till was overconsolidated with an OCR of about 10, which means that the preconsolidation margin was about 1,000 kPa at about 7 m depth. Triaxial tests indicated a 29° internal friction angle and an earth stress coefficient at rest, $K_0$, equal to 1.5 (N.B., before pile driving).

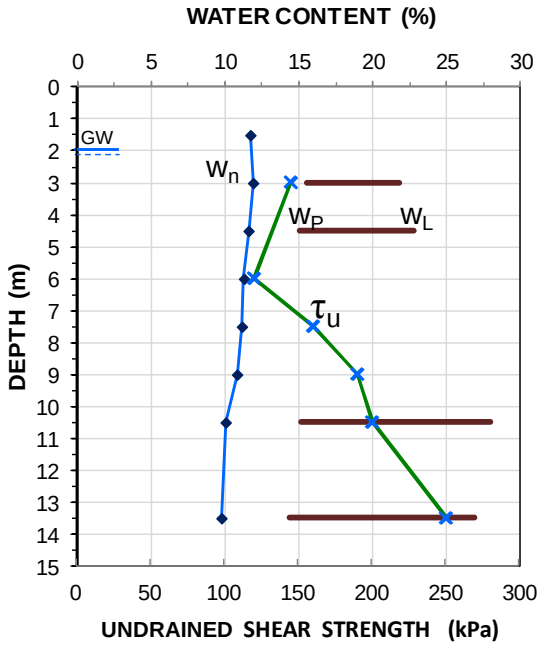


Figure 1A. Water content and undrained shear strength

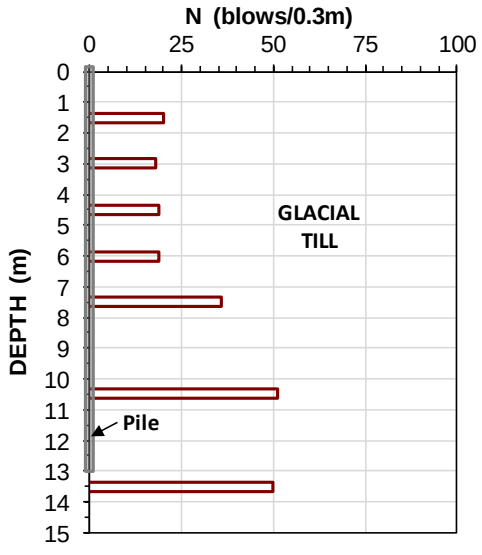


Figure 1B. Distribution of SPT N-indices

The site investigation included two screwplate tests employing a 160-mm wide screwplate at depths of 3 and 6 m. Figure 2 shows the stress (kPa) versus movement (% of plate diameter). I find it convenient to model—to fit—mathematical functions to the load-movement curves of footings, plates, and piles (Fellenius 2014a). Details on five such functions are appended to this paper. I have performed a best-fit of the 6-m depth screwplate test-curve to the Ratio Function (Eq. A1 in the Appendix obtained for an exponent, Θ, of 0.600).

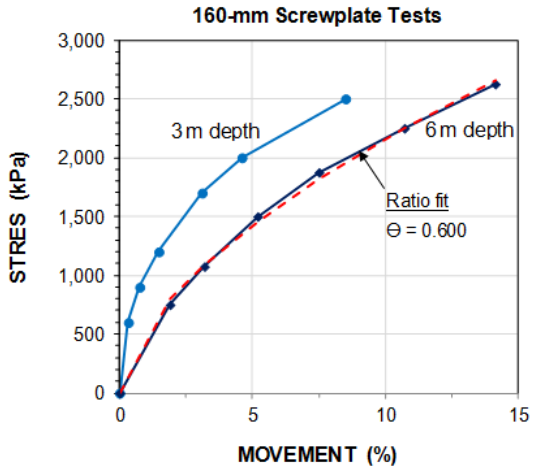


Figure 2. Stress-movement curves of the screwplate tests

Figure 3 shows the results of the static loading tests as the measured load-movements for the two test piles. The method of testing was quick tests consisting of sixteen 85-kN and twenty-three 90-kN increments of load to maximum loads of 1,360 and 2,080 kN, respectively. The piles reached a plunging response at the maximum loads of 2,080 and 1,360 kN, respectively. The authors interpreted the load-movement curves to indicate total pile capacities of 1,160 and 1,780 kN, respectively.

As based on the at the time common assumption of toe resistance being 9 times the undrained shear strength (220 kPa at the pile toe depth), the authors estimated a unit toe resistance of 2 MPa, which gave total toe resistances of 90 and 160 kN, respectively, for the H420 and H800 test piles. By subtracting the toe resistance from the interpreted pile capacities, the authors determined the shaft resistance, to be 1,070 and 1,620 kN, respectively.

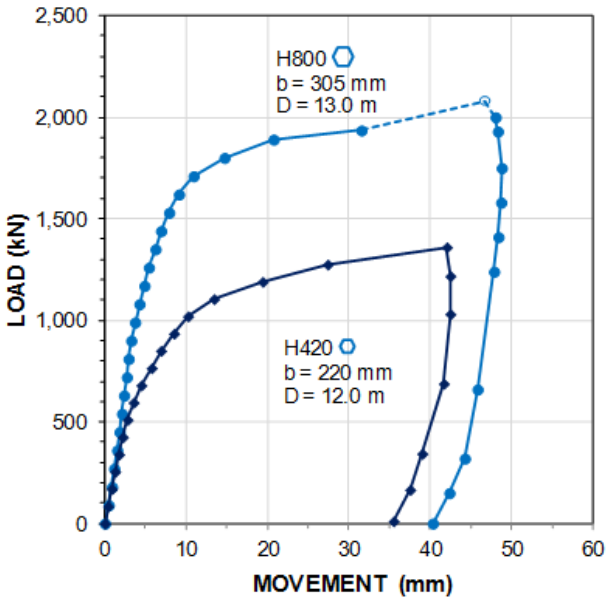

Figure 3. Pile loading-test load-movement curves

The authors also applied the earth stress coefficient and the friction angle to calculate the effective stress proportionality coefficient (ß = $K_0$ tan φ') to 0.7, resulting in the alternative shaft resistances of 1,200 and 1,850 kN, respectively, for the two piles. In a third approach, applying 170-kPa average undrained shear strength along the piles times an alpha-factor of 0.45, the authors obtained total shaft resistances of 700 and 1,060 kN, respectively.

Thirty years ago, there were no suitable computer programs for analyzing results of a static loading test nor, for that matter, to simulate or model one. Today, however, we can deliver a complete analysis with minimal effort. Such work has shown that capacity is far from a precise concept for expressing the response of a pile to load. This was, for example, illustrated in the results of two recent pile prediction events (Fellenius 2013a; 2014b), where capacities determined from load-movement curves hit all over the place.

Pile shaft resistance response is rarely elastic-plastic, but either strain-hardening or strain-softening. The latter is prevalent in clays, even in dense glacial clay tills. Pile toe resistance, on the other hand, is never plastic, that is, it never shows a specific capacity, but takes the form of a strain-hardening curve with increasing movement for increasing load, much like the response shown for the mentioned screwplate test.

When performing a back-analysis of observed load-movement response, one must realize that the response is governed by effective stress distribution along the pile and that the analysis is better performed applying the ß-method (effective stress method), as opposed to the α-method (total stress method).

As mentioned, the load-movement response of both the pile shaft and the pile toe can be simulated using simple relations, called t-z and q-z functions. The pile toe q-z response is usually best simulated by the Ratio Function (Eq. A1 in the Appendix) and depends then on the value of the exponent, which typically ranges between about 0.4 through about 0.9 (an exponent of 1.0 signifies a linear load-movement relation). For the subject tests, I assigned the same Ratio Function (Θ = 0.600) to the pile toe as that I found fitted the screwplate at depth 6 m. Meyerhof et al. (1981) did not report for which toe movement that they considered the toe resistance to have been mobilized. When applying an "ultimate" toe resistance, I have often found it practical and useful to consider this to have been reached at a 30-mm toe movement and I, therefore, applied this movement for the toe resistance.

I input the characteristic shaft resistance as equal to the balance after subtracting the toe resistance for the 2-MPa toe stress, which gave ß-coefficients equal to 1.0 and 1.3 above and below 7 m depth, respectively. After a series of trial-and-errors, I obtained a fit to the load-movements measured for Pile H800, using the Hyperbolic t-z function (Eq. A2 in the Appendix) with the 100-% value assumed mobilized at a 5.5-mm relative movement between the pile shaft and the soil and a Slope C1 equal to 0.0090 (which corresponds to a 111 % resistance at infinite movement).

For Pile H420, I tried using the same input (only changing to the smaller size of the pile), but found that I needed to increase the ß-coefficient in the upper 7 m to 1.1 and lift the toward-end-of-test load-movement curve by decreasing the t-z Slope $C_1$ to 0.0083 (which corresponds to a 120 % resistance at infinite movement). The changes are minimal (choosing a ß of 1.05 and a $C_1$ of 0.0086 for both piles would have produced slightly less good, but fully acceptable fits to the measured curves.

Figures 4A and 4B show the calculated pile-head load movement curves together with the measured curves for Pile H800 and H420. As seen, the agreement between calculated and measured is good. The figures also show the calculated toe and shaft resistance load-movement curves, resulting from the same calculations. In both figures, the line from the 30-mm pile toe movement intersecting the pile head load-movement curve indicates the magnitude of the applied load that produced the 30-mm toe movement. (The movement difference is the pile shortening). As mentioned, this load can be defined as a toe-movement-deduced pile capacity. For reference, the Offset Limit load is indicated. Note that the simulation does not include any consideration for potential residual load, which may or may not have affected the load-movement response.

For both fits, the primary imposed restriction was that the pile toe movement q-z function was the Ratio Function with a 0.6-exponent and that the toe resistance mobilized for a 30 mm movement was equal to the authors' stated toe resistances. The authors determined the toe resistance value by applying a coefficient to the undrained shear strength of the very dense, overconsolidated glacial till. In my opinion, that approach is uncertain even for soft marine clays, for which it was originally developed. The glacial till is a clay till, that is, it has more than thirty percent of clay-size particles. However, the remaining portion consists of silt, sand, gravel, and cobbles, and the measured water content shows that the density is close to that of concrete. In my experience, the toe resistance must have been greater than the value stated by the authors, and I would expect a much stiffer toe resistance and a value at least equal to, but probably even larger than 10 MPa to be mobilized at a 30-mm toe movement. Moreover, I would expect that the shaft resistance would show a strain-softening response as opposed to a strain hardening or plastic response.

I repeated the analysis with a toe resistance of 13 MPa, still assumed valid for a 30-mm toe movement and applied a load-movement curve per the Ratio Function with a 0.6 exponent. For the shaft response of Pile H800, I applied ß-coefficients of 0.8 and 1.1 above and below 7 m depth, respectively, and the Hansen Function for the shaft resistance t-z response with a 5.5-mm movement for the peak force and a $C_1$-slope of 0.002. For Pile H420, but for changing the input of movement for the peak force to 6.0 mm, I applied the same parameters to the fitting of the calculated pile-head load-movement curve, again finding that the two piles responded almost identically. Figures 5A and 5B show the results of the piles for the stiffer toe resistance. The main consequence of using the stiff resistance instead of the authors' small toe resistance is the significant strain-softening that becomes necessary in order to counter the increasing toe resistance with the movement. In my experience, the clay till would trend to a such strain-softening response.

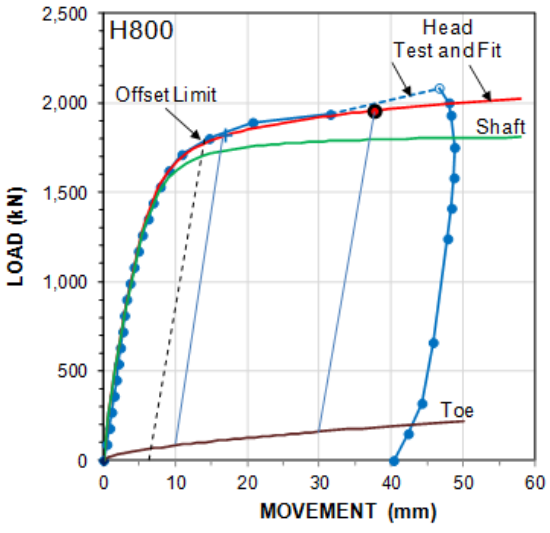


Figure 4A Pile H800 load-movement curves for authors' stated toe resistance

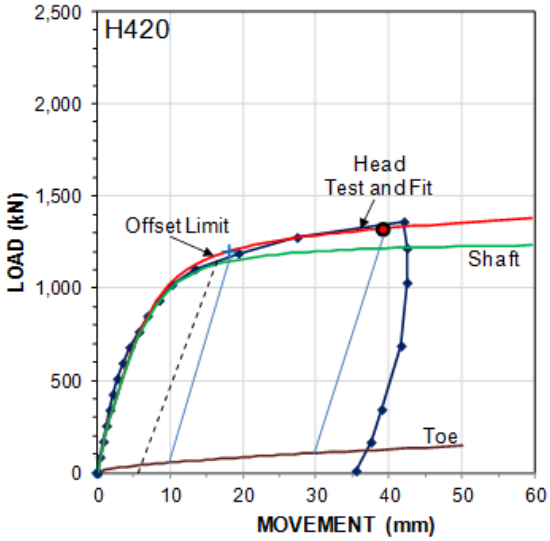


Figure 4B Pile H420 load-movement curves for authors' stated toe resistance

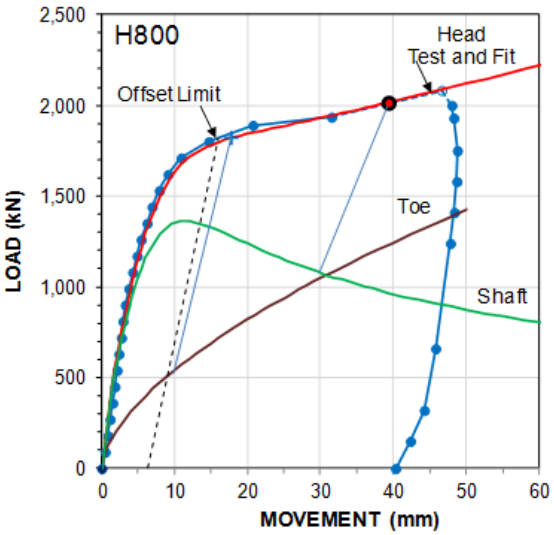


Figure 5A Pile H800 load-movement curves for stiff resistance

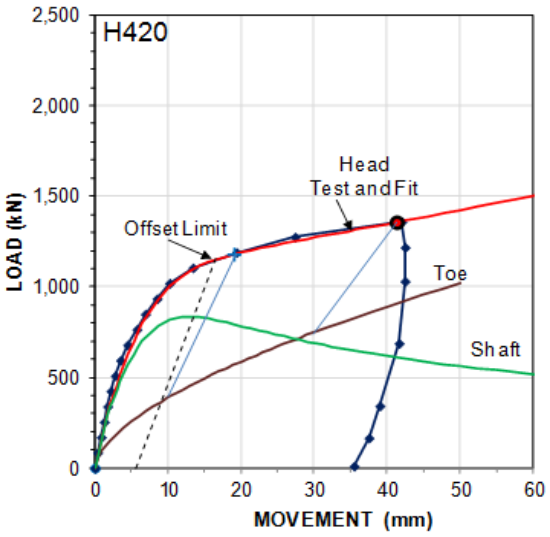


Figure 5B Pile H420 load-movement curves for stiff resistance

For Pile H800, the fit to the stiff toe resistance results in a total shaft resistance, $R_s$, and a total toe resistance, $R_t$, of 1,380 and 1,050 kN, respectively. The sum is 2,420 kN, which is much larger than the maximum test load and the pile capacity one would eyeball from the test curve. The reason is that $R_s$ is the sum of the peak resistance for each pile element, occurring for about 6 mm movement. The pile head movement is 12 mm when the pile element nearest the pile toe has reached its peak value. In contrast, $R_t$ is the toe resistance occurring at a 30-mm toe movement, when the shaft resistance has reduced to about 1,000 kN. This demonstrates that the pile capacity determined as the sum of the maximum shaft resistance of a series of pile elements is not the capacity one would interpret from the pile head load-movement curve. This is often not recognized in the evaluation of the results from an instrumented test, where the pile element response is established from the results of strain-gage measurement at different depths and, indeed, often used as representative for the "pile capacity".

Moreover, as the pile is not rigid, the simulations include the pile axial stiffness, EA, which is applied to the calculation of the Offset Limit Line (dashed line in the figures). The two sloping thin solid lines rising from the 10-mm and 30-mm pile toe movements to intersect with the pile-head load-movement curve show the shortening of the pile for these test loads. At first thought, one would expect the slopes to be parallel to the Offset Limit Line (slope parallel to the elastic line), but this would only be true in the rare case of ideally plastic ultimate shaft resistance. The fact that the shortening slope is not a straight line is taken into account for the line connecting the pile-toe movement to its associated pile-head load. Again, this strain-softening effect (as well as the strain-hardening) needs to be considered in the evaluation of the results of strain-gage instrumented static loading tests. Otherwise, when the shaft response is strain-softening, the stiffness evaluation method called the "incremental-stiffness method" or "tangent-modulus method" (Fellenius 2014a) will result in a too drastic reduction of the stiffness with increasing strain. Similarly, for evaluation of strain-gage records from pile tests in strain-hardening soil, the result can actually appear to suggest a progressively increasing axial pile stiffness.

Which of Figures 4 and 5 shows the correct shape of the shaft and the toe load-movement curves? I may have a preference for the simulation that applied the stiffer toe response. But, in all fairness, no one knows the answer to the question: does the pile have a soft toe response or a stiff? The answer would require testing piles of different length and/or testing instrumented test piles. Or, performing bidirectional tests, or combining static tests and dynamic tests, which methods will be addressed later in this presentation.

If the soil settlement around the pile is small enough to be disregarded, then, the foundation settlement will be limited to the pile toe movement and the shortening of the pile for the pile load. Most piled foundations will perform adequately if the pile toe movement is smaller than 10 mm. For the subject case, as the long-term settlement of the glacial till will be minimal, the pile settlement will be negligible. This is demonstrated in Figure 6A, which shows the short-term and long-term distributions of load in the pile for the alternative of the stiff pile toe condition. The curve marked "short-term" is the distribution developing immediately after completion of the structure supported by the piles. The one marked "long-term" is the distribution characterized by the shaft resistance being fully mobilized in the negative direction (downward) along an upper length of the pile and, then mobilized in the positive direction (in this case, the transition zone is assumed to be rather long due to the small soil settlement around the pile). Because of the small pile toe penetration, the toe resistance is only a small portion of the resistance otherwise available in the till. The pile toe load-movement response is plotted at the bottom of the load-distribution graph. The simulations are performed by the UniPile software (Goudreault and Fellenius 2013).

If, however, the surrounding soils would be compressible and less preconsolidated, and appreciably affected by regional subsidence, adjacent foundations loading the ground, fills, groundwater lowering, etc., then, the soils will settle and the piled foundation will be affected by downdrag. The effect of the downdrag will be an increased axial pile load and an increased load at the pile toe, which will result in an increased pile toe movement. Figure 6B shows the long-term conditions for Pile H800 and the case of stiff pile toe response. For such cases, it is vital that the pile-toe load-movement response be determined and considered in order to produce a safe and reliable design. Moreover, the about 40-mm foundation settlement in the latter case might not be acceptable for the structure supported by the foundation. Note, however, that the pile "capacity" has not changed (the pile head load-movement curve is the same), so the factor of safety is the same, but Case A is "safe" and Case B may not be due to excessive downdrag. Capacity is a very undefined and diffuse concept that is really not suitable for use in serious design and should be replaced—or, at least, be supplemented—by performing analysis of the pile deformation and of the soil and foundation settlement.

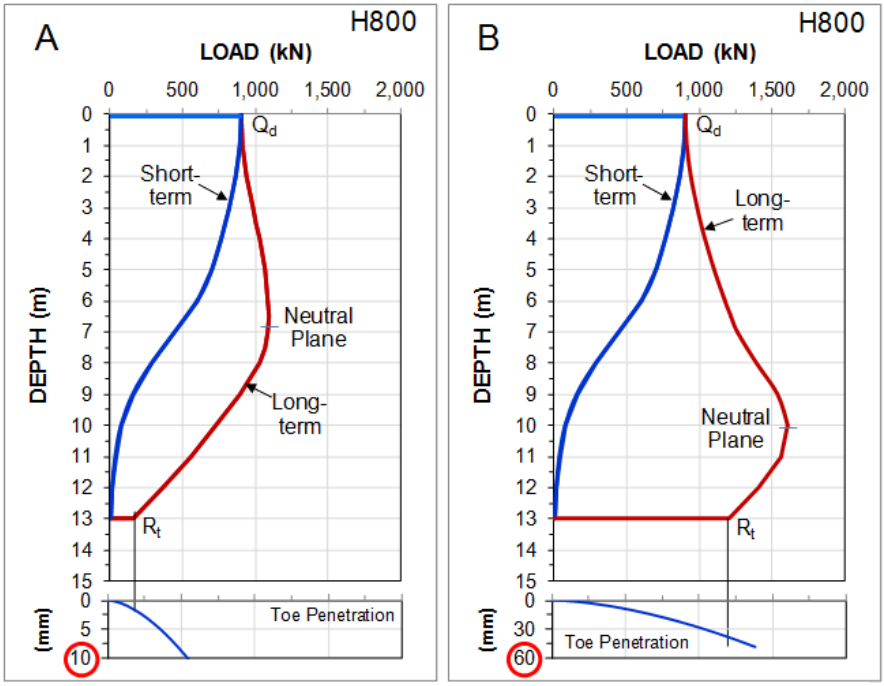


Figure 6 Short and long-term load distributions for the stiff pile toe condition
(A) negligible settlement of the soil around the pile
(B) considerable settlement of the soil around the pile

## 2.2. Bidirectional Test

As the analysis of the 1981 example shows, the head-down load-movement curve itself does not provide much useful information on the resistance distribution and the pile toe response. It is easier said than done to accurately separate the shaft resistance response from the toe resistance response. Yet, the latter is the most important information required for the design of a piled foundation. This difficulty can be avoided by performing a bidirectional test (Elisio 1983; 1986, Osterberg 1989, 1998) instead of the conventional head-down test. Figures 7A and 7B show the results of simulated bidirectional tests on Pile H800 for the soft and stiff toe responses with test cell placed at 9.5 and 12.0 m depth, respectively, which are "ideal positions" (force equilibrium locations, calculated using UniPile software). Because the strain-softening shaft response for case of stiff toe response is often difficult to record—the pile plunges—, in Figure 7B, the progress of the upward portion is shown dashed after the peak shaft resistance was reached.

As demonstrated, the bidirectional test takes much of the guesswork about the resistance distribution out of the test analysis. Moreover, fitting a back-calculation analysis to test records from a bidirectional test are much easier than fitting to records of a head-down test. If desired, after such a fit is completed, a conventional head-down load-movement curve (Figures 4 and 5) can be produced by suitable software for comparison to a display of results of an actual conventional head-down test.

Bidirectional tests were performed at a site in Sao Paolo, Brazil (Arcos 2014) on two Omega Piles (Drilled Displacement Piles, DDP, also called Full Displacement Piles, FDP) both with diameter 700 mm and embedment 11.5 m. Pile PCE-02 was provided with a bidirectional cell level at 7.3 m depth and Pile PCE-07 at 8.5 m depth. The bidirectional cell assembly was attached to the reinforcement cage that was inserted into the fresh concrete. The concrete had been placed per the usual procedure for the pile type (during the withdrawal of the drilling equipment). Figure 8 shows the soil profile, SPT N-indices from boreholes drilled next to the two piles, the depth to the groundwater table, and the location of the bidirectional cells. The soil consisted for the most part of silty sand and was loose to compact down to about the location of the cells and dense below the cell depths. At the pile toe, the soil was stated to be very dense. The maximum test load applied by the cell assembly was about equal to the desired working load on the piles. Both static loading tests were by applying load increments of 42.3 kN every ten minutes to a maximum of load of 932 and 732 kN for Piles PCE-02 and PCE-07, respectively. For Pile PCE-02, the maximum load was held for 60 minutes.

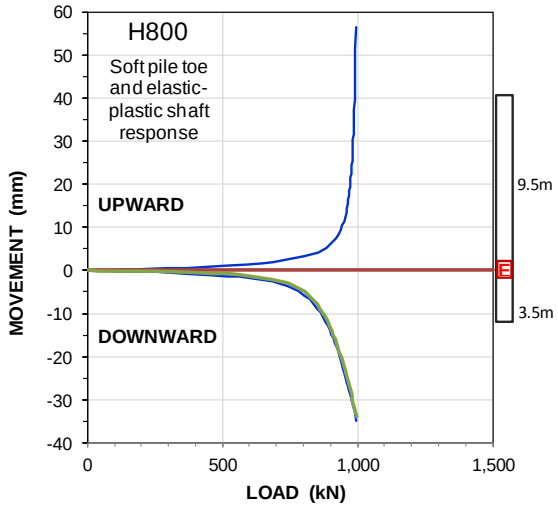


Figure 7A Results of bidirectional tests simulated as performed on a Pile H800 responding per the authors' soft toe assumption

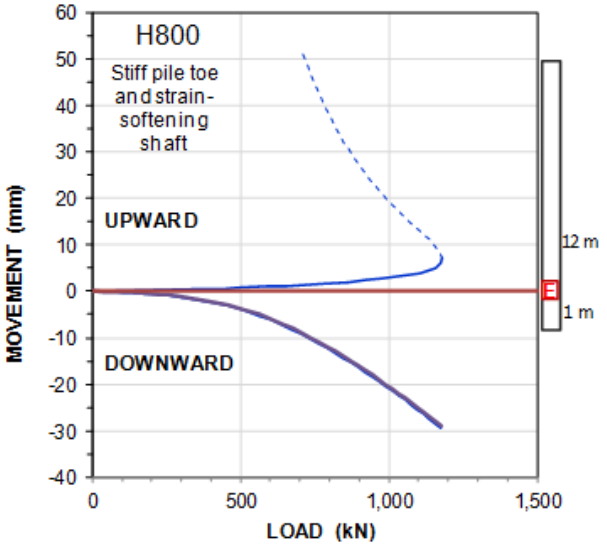


Figure 7B Results of bidirectional tests simulated as performed on Pile H800 responding per my stiff toe assumption

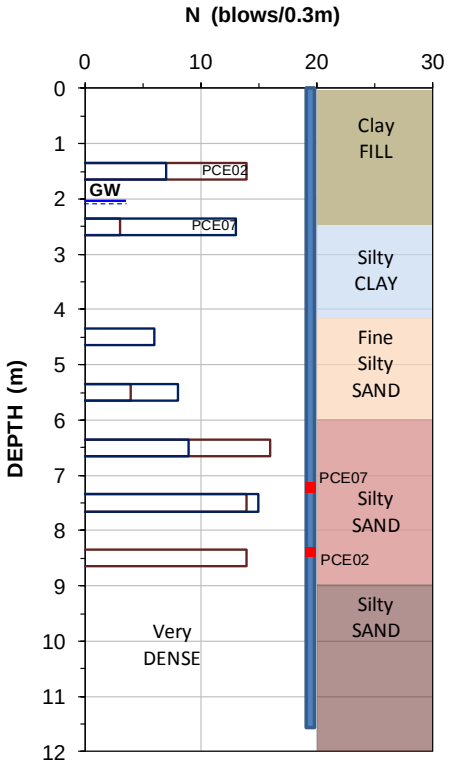


Figure 8. Soil profile at the CFA site with N-index distribution from two adjacent boreholes

The results of the bidirectional tests on Piles PCE-02 and PCE-07 are shown in Figures 9 and 10, respectively. The upward curve represents the measured upward movement of the pile head and the downward curve the measured downward movement of the base of the bidirectional assembly. I have fitted simulated load-movement curves to the measured curves for both tests employing an effective stress back-calculation. The input to fit to the results of Pile PCE-02 showed to be similar to what usually will establish a fit to measured values for the FDP pile: the beta-coefficients were 0.4 to 2.5 m depth, 0.6 to 6.0 m depth, and 0.9 to the cell level and below. The toe resistance, $r_t$, was 3 MPa. The shaft resistance values were assumed to be mobilized at a 5-mm relative movement (δ), whereas the toe resistance was assumed to require a 30-mm movement of the pile toe. The Ratio Function was used in simulating both the t-z and q-z functions. The symbol Θ in the figure stands for the Ratio Function exponent. The distributions are adjusted for the buoyant weight of the pile portion above the cell level and the pore pressure acting on the cell assembly base.

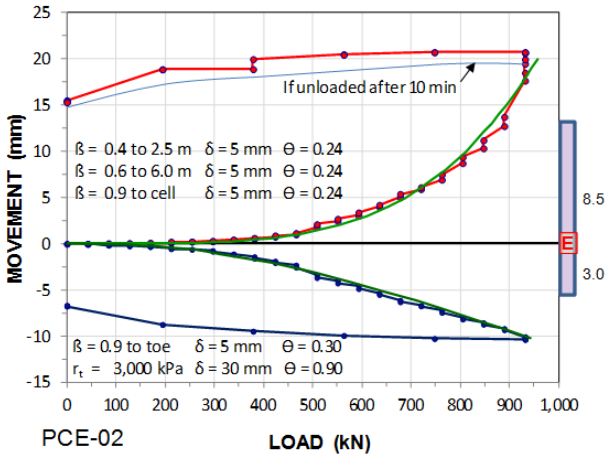


Figure 9 Results of bidirectional test on Pile PCE-02

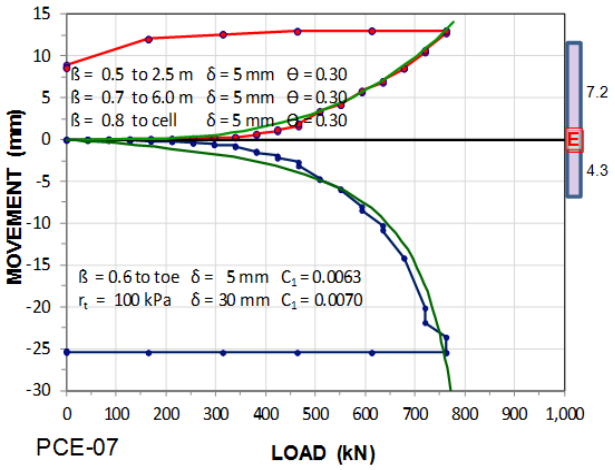


Figure 10 Results of bidirectional test on Pile PCE-07

A similar input was used to fit to the upward results of Pile PCE-07. However, to achieve the downward fit required assuming a smaller ß-coefficient with a Hyperbolic t-z function and for the pile toe with a $C_1$-coefficient of 0.0073, which means a slightly more curving shape of the shaft shear load-movement curve than that of the Ratio Function used for Pile PCE-02 (a $C_1$ of 0.0073 corresponds to a 137 % resistance at infinite movement). More important, the fit required almost no toe resistance, only 100 kPa. An analysis for a 1.0 m shorter pile with a ß-coefficient the same as above the cell level and no toe resistance gave a fit as good as the one showed in the figure. It is quite clear that the bidirectional test has revealed that the construction of the pile had failed to provide an acceptable toe condition.

Ordinarily, for shaft resistance of bored and driven piles, the t-z response is found to be more similar to a plastic response, e.g., the

Hyperbolic or Exponential response, as opposed to that for the Ratio Function. However, I have seen results of fits of shaft resistance to the somewhat stiffer response which is usually represented by the Ratio Function also in other analyses of the results of tests on FDP piles.

In my opinion, the bidirectional test is superior to the conventional head-down test. Loosely stated, this is because the bidirectional test provides the response to load in two points, at the pile head and at the location of the cell, as opposed to just at the pile head. More rationally expressed, the bidirectional test, properly designed, provides the pile-toe response, which, as illustrated above (Figures 6A and 6B) is necessary for assessing the settlement of a piled foundation. Moreover, as will be addressed further on, the load in the pile at the cell location established by the bidirectional cell assembly is unaffected by residual load (locked-in load) in the pile, which otherwise is difficult to ascertain. For example, if residual loads are present in the pile at the test occasion, they will affect the loads determined from strain-gage instrumentation and the true load distribution and pile response of a head-down test will be difficult to determine.

Figure 11A shows the load distribution in the two test piles. The toe resistances shown are the values obtained for the actual maximum movement in the test, about 10 mm for Pile PCE-02 and 25 mm for Pile PCE-07. The fact that the curves are more or less parallel down to the pile toe demonstrates that the pile shaft resistances are essentially equal. However, as shown, the toe resistances are not; the toe resistance for Pile PCE-07 is very small. This is further emphasized in Figure 11B showing the pile-toe load-movement response (plotted using the same load scale as in Figure 11A).

Many desire a direct comparison between the conventional head-down test and the bidirectional test because the results of a head-down test are usually assessed from the pile-head load-movement curve. If desired, an equivalent head-down load-movement curve can easily be constructed from the results of a bidirectional test. The usual approach to construct the equivalent curve is first to add the cell loads for equal measured movements up and down. The load causing the downward

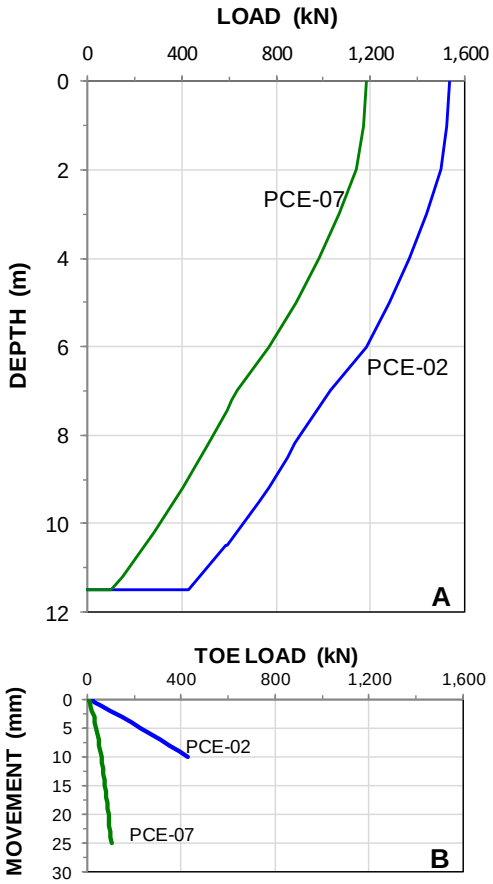


Figure 11 Piles PCE-02 and PCE-07 load distributions
A. Load distribution versus depth
B. Pile toe load-movement relations

movement in the equivalent test in reaching down to the cell level will have caused 'elastic' shortening of the pile, i.e., additional movement, which is added to the measured movements. This is not fully correct, however, the so determined equivalent curve disregards the fact that the bidirectional test mobilizes the shaft resistance along the length immediately above the cell level first and the shaft resistance nearest the ground surface last. The soil near the cell is usually stiffer than the soil near the ground surface, which the conventional head-down test mobilizes first. The latter is difficult to adjust for when determining the equivalent head-down load-movement curve directly from the measured values of load and movement at the cell. This complication is avoided by first simulating the bidirectional test as shown above. On having achieved the fit to the test data, the simulation of the head-down response is provided by the same software algorithm (UniPile in the subject case).

The results of the simulation of the equivalent head-down load-movement curves for the two piles are shown in Figure 12. The figure is supplemented with the pile shortening curves. The measured maximum movements upward and downward for the measured bidirectional test are indicated in the figure. It can be argued that the equivalent head-down curve is "measured" as long as the smallest of the maximum movements is not exceeded. The dashed curve extensions are extrapolations of the "measured" values. In a bidirectional test, where either the upward or the downward response has shown small movement, the equivalent curve then becomes mainly an extrapolation. This can be avoided by continuing the test to the maximum capacity of the bidirectional cell either in load or movement (opening of the cell) as opposed to terminating the bidirectional test at a predetermined cell load, usually the desired working load, which now is the common approach. Such premature termination is far too common because the bidirectional test is considered to be a replacement for the conventional test to twice the desired working load disregarding the fact that it is a test method providing much more information and possibility for establishing the pile response better than the conventional test can offer—and disregarding that continuing the test adds no extra costs to a project. All bidirectional tests should, of course, be carried to the minimum load required for the project, but the tests should then continue to the limit of the cell assembly.

A bidirectional test is usually designed to locate the cell at the "balance point" between fully mobilized upward and downward load-movements, i.e., located so as to provide the "ultimate" response for the entire length of the pile. If successful in this, the equivalent head-down load-movement curve will be true to the measurements up to a load equal to about twice the maximum cell load. However, this is difficult thing to achieve. Often, the test will not provide sufficient information for one or the other direction. For routine proof-testing, this is normally no problem because an equivalent pile-head load-movement curve will still show an adequate maximum load, allowing for assessing whether or not the pile is

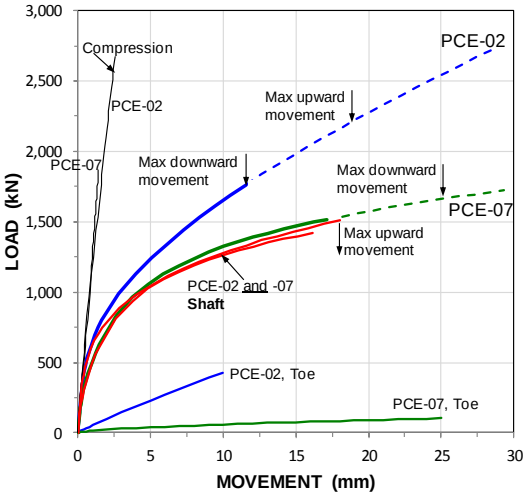


Figure 12 Equivalent head-down load-movement curves for Piles PCE-02 and PCE-07

acceptable (although it will be on the extrapolated part). However, not much else is learnt from the test. It is more useful to plan the test with the cell placed two or three pile diameters above the pile toe so as to ensure that the downward response is well determined. Then, it is easy and inexpensive to perform a tension test ("pull" test) on the length above the cell, which will establish also the true and full response of the length above the cell assembly. By fitting the results to an effective stress analysis and converting the fitted condition to an equivalent head-down load-distribution curve, or an equivalent head-down load-movement diagram, the full response of the pile is established.

## 2.3 Combining static and dynamic tests

Piles can also be tested by means of dynamic methods, which method is not limited to just driven piles (Goble et al. 1980). Oliveira et al. (2008) reported a case history from Sao Paolo, Brazil, where dynamic tests were performed on a 700-mm diameter, 12 m long, CFA pile 66 days after constructing the pile. The results were verified by carrying out a static loading test 31 days after the dynamic test. As shown in Figure 13, the soil profile was composed of a upper 4 m thick layer of silty clay with sand followed by about 4 m of alluvial soil consisting of organic soft silty clay and sand, which was deposited on a sandy residual soil continuing to depths deeper than 12 m.

The detailed dynamic test data (the CAPWAP results) were received by personal communication with Mr. Sergio C. Paraiso, Geomec, Brazil.

The dynamic tests followed the procedure of Aoki (2000) called dynamic increasing energy test, DIET, consisting of a succession of blows from a special free-falling drop hammer, while monitoring the induced acceleration and strain with the Pile Driving Analyzer. Five blows were given with an 8,000-kg hammer and heights-of-fall of 200, 400, 600, 800, and 1,000 mm, respectively. Each blow was analyzed by means of the CAPWAP program (Rausche et al. 1985).

The static loading test was carried employing 14 load increments to a maximum load of 2,700 kN. The load-holding duration was not mentioned in the paper, but stated to be using a "*slow loading up 1,620 kN and, thereafter, to the end of the test (2,700 kN), fast loading*". The six first "slow" increments were 270 kN and the following eight "fast" increments were about 118 kN.

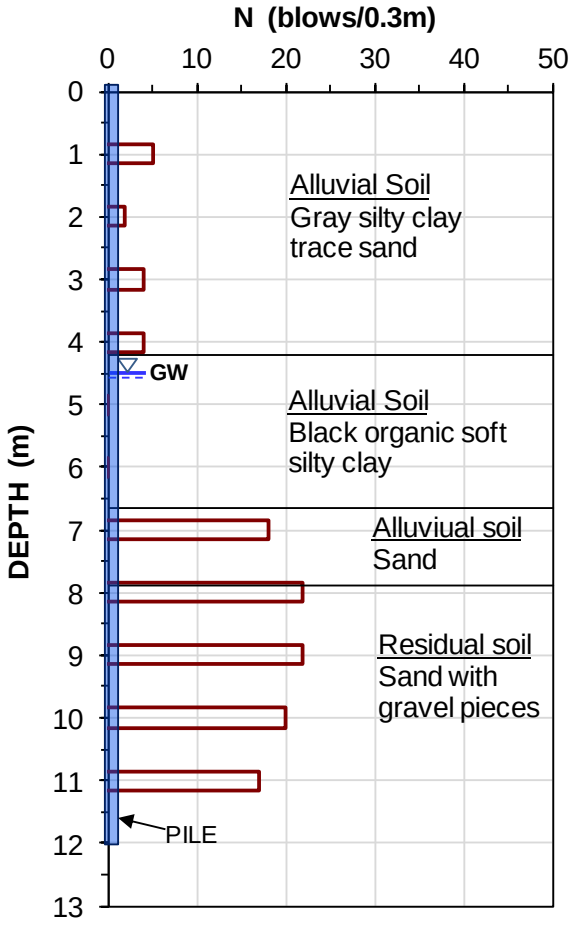


Fig. 13 Soil profile and N-indices at the CFA pile site

Figure 14 shows the load-movement curves of the first three dynamic tests (CAPWAP determined) and the static test plotted in sequence. The curves for Blows 4 and 5 are not shown because the analyses show that the fourth and fifth blows were affected by the preceding blows which resulted in a temporary break-down of resistance associated, probably, with development of excess pore pressure—the shaft resistance reduced and the toe resistance did not increase despite the about 30-mm additional pile toe penetration. The pile capacity at the time of the dynamic tests was essentially reached in the third blow at the 20-mm total pile penetration. The additional penetration of the pile toe, I assume resulted in the small increase in the toe resistance marked as "qz" in the figure.

The DIET test assumes that CAPWAP-determined static load-movement curves represent a series of loading-unloading, and reloading of the pile as in a static loading test to a progressively larger maximum applied load. The curve from the first blow represents virgin condition and the following two blows represent reloading condition. The dashed line approximately combines the curves into the load-movement curve for a static test with no unloading/reloading. I have aimed it toward the beginning of the CAPWAP-determined capacity for each blow (as opposed to the capacity toward the end of the CAPWAP-determined simulated load-movement curve suggested by Aoki 2000).

The load-movement curve of the static loading test shows a steep initial rise which, as indicated, is the same shape as that for the CAPWAP curve of the third blow, indicating the re-loading response of the pile. Note that for the loads beyond the CAPWAP-determined capacity, the curve showed a less steep response.

When comparing capacities mobilized in a dynamic test to that mobilized in a static loading test, the reference is the Offset Limit (Davisson 1972). Otherwise, what capacity the static test shows is a function of the user's preferred definition of such. My own preferred value is the pile head load that moved the pile toe 30 mm.

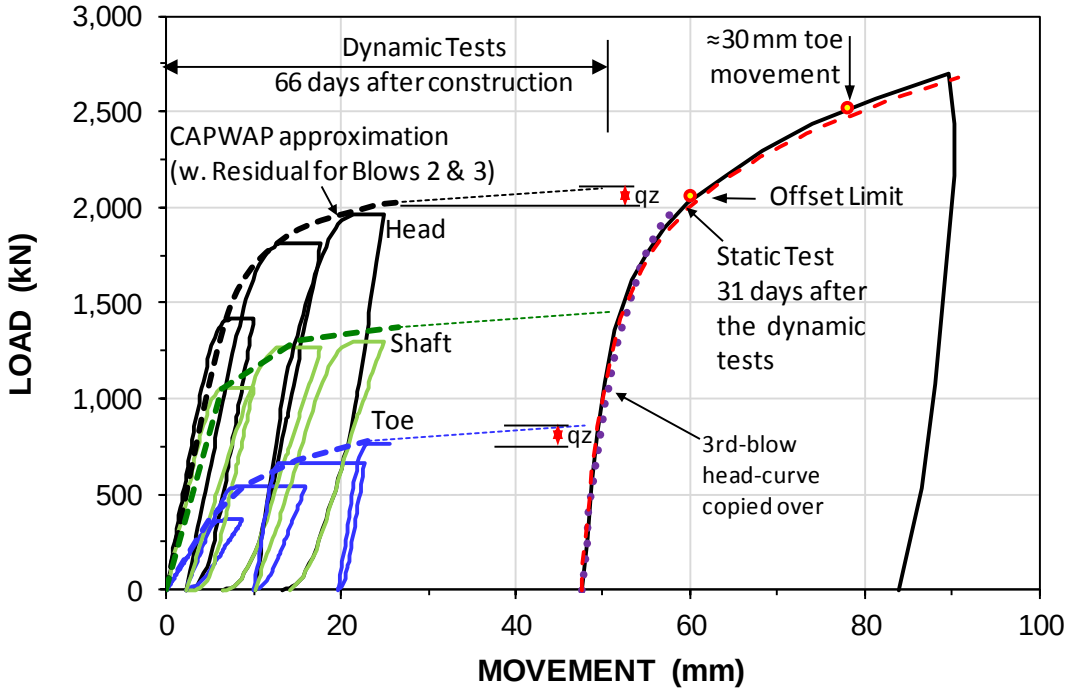


Figure 14 Load-movement curves for the five CAPWAP analyses and the static loading test

Some continued increase of shaft resistance might have developed due to set-up during the next 31 days of wait after the end of the dynamic testing to the start of the static test. However, the assumed increase of toe resistance ("qz") show in the figure is enough to account for the slight increase of pile capacity evidenced in the static test.

The dynamic testing resulted in a 50-mm advancement of the pile by the hammer blows, which will have built in load in the pile, so-called residual load. Residual load was first shown to be a reality by Nordlund (1963), Hunter and Davisson (1969), and Gregersen et al. (1972). The mechanism is now well-established. That it is still often overlooked in engineering practice is therefore surprising. Based on past analyses, I made the assumption that the dynamic tests resulted in a residual load (built up of a shaft resistance amounting to 70 % of the resistance developed for a 5-mm relative movement between the pile and the soil) combined with a toe resistance equal to 40 % of the resistance mobilized at a 30 mm virgin toe movement. (It is worth mentioning that the CAPWAP-determined static load-movement curves would also be affected by presence of residual load in a test pile).

I assumed beta-coefficients equal to 0.40, 0.25, and 0.60 for the subject three soil layers, respectively (the values are smaller than those chosen for the previous case history because shaft shear is normally smaller for CFA piles as opposed FDP piles). A trial-and-error process, resulted in a t-z curve for the fit to the static test curve for a t-z Hyperbolic Function with a $C_1$-coefficient of 0.0080 (corresponds to a 125 % larger shaft resistance at infinite movement). For the pile toe, I input a unit toe resistance of 2.5 MPa and a q-z Ratio Function with 20-mm for 100 % of load movement and an exponent of 0.60. I decided on these values in recognition of the residual load condition. For virgin conditions, to allow for the softer soil stiffness, I changed the t-z function to a 5-mm 100-% movement and a $C_1$-coefficient of 0.0070 which makes for a slightly less steep rise of the shaft resistance curve and a 30-mm 100-% movement for the q-z Ratio Function. The results of the calculation for the virgin condition—no residual load—are included in Figure 15, which shows the static test load-movement curves. The figure also includes the shaft and toe load-movement curves for the virgin condition and the CAPWAP load-movement curves for the first blow.

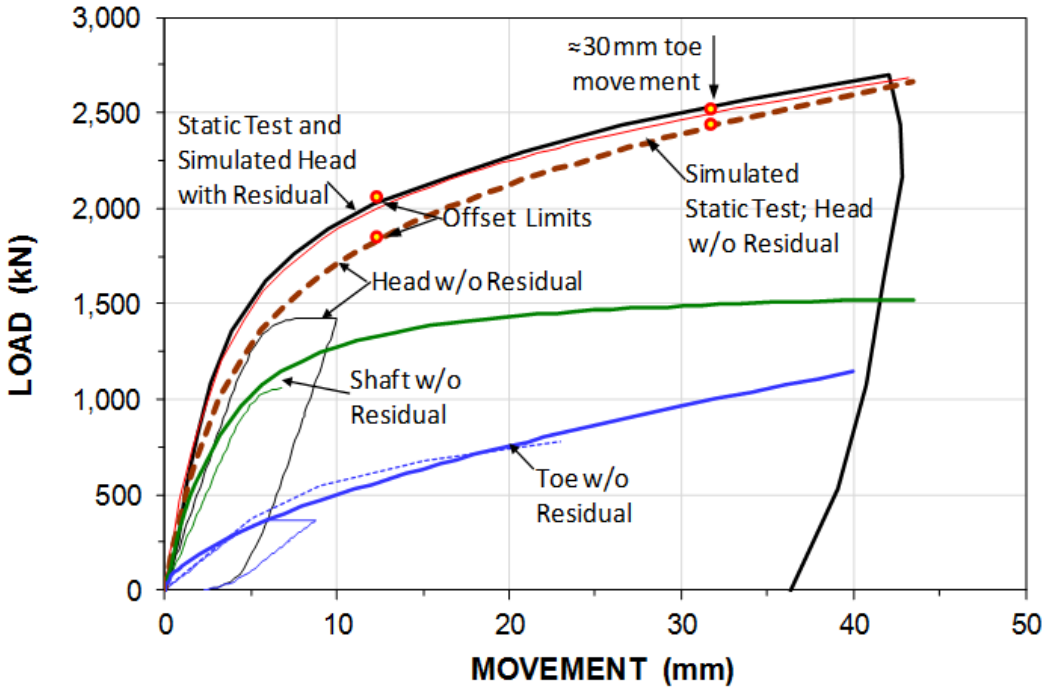


Figure 15 Load-movement curves for the pile head with residual load and simulated curves for the pile head with residual load and for the pile head, shaft, and toe without residual load and the CAPWAP-determined load-movement curves from the first blow

The simulated pile-head curves shown in Figure 14 agree well with the gradual progress of the CAPWAP-determined pile-head curves as well as with the measured static test curves. The simulated curves for the pile shaft and pile toe agree well with CAPWAP-determined pile shaft and pile toe curves. The fact of the agreement is not a definite proof that the input represents the actual conditions for the soil and the pile. However, some credibility rests with the fact that the fit to the test is made with input of residual load, whereas the curves calculated for the virgin conditions, having the same soil input but for the allowance of the larger movements agree well with the CAPWAP-determined curve from the first blow, which also was for virgin conditions.

The analysis results show that the CAPWAP-determined pile capacity agreed very well with the capacity of the static loading test, when defined by the offset limit. The results also show that the dynamic tests stiffened up the pile giving an increase of the capacity determined from the load-movement of the static loading test. The increase was about 200 kN or 10 %.

The DIET method of dynamic testing provides results that more closely resemble those of a static loading test. The DIET test could build in residual load in the pile, which could result in a pile capacity slightly larger than that obtained in a static loading test for virgin conditions test. If a simulation of results from a DIET test with reasonable assumption of residual load distribution is carried out, it could then be used to simulate the somewhat less stiff response for the virgin condition. However, if capacity is defined not by the offset limit, but at large deformation, the effect of any residual load is much diminished and of little concern.

The presence of residual load particularly influences the load distribution, giving an exaggerated value of the shaft shear along the upper portion of the pile and a smaller than actual shaft shear along the lower portion. The toe resistance can appear very much smaller than actual. This is illustrated in Figure 16, which shows the "true" load distribution and the distribution of residual load for the analyzed pile. If the pile had been supplied with strain gage instrumentation and the strain imposed in the test had been believed to be the only

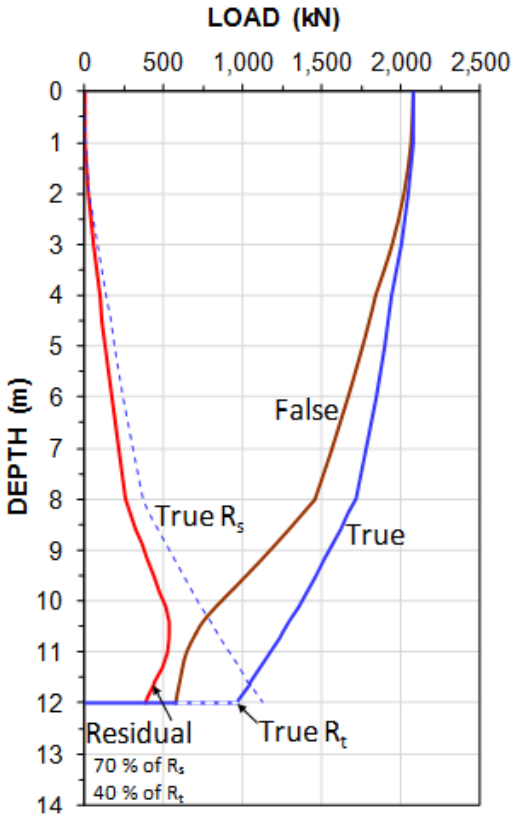


Figure 16 Load distributions for true and false conditions with residual load distribution

response to the applied load, the "false" resistance would have appeared. An extrapolation of the test results to select longer or short piles would then have been very much in error.

## 2.4 Test on a jacked-in cylinder pile

Glostrext Technology (2013) reported results of a cylinder pile constructed in Singapore. The soil profile consisted of sandy and gravelly silt of the Bukit Timah formation, which is a weathered in-place, granitic soil. The groundwater table was close to the ground surface. The pile was a pretensioned, 600-mm diameter spun-cast pile with a 150-mm thick wall installed to 15-m embedment depth by hydraulic jacking. The jacking was terminated when the load reached 5,760 kN (probably surpassing it by a small margin). No measurements of load and penetration were taken during the installation-jacking of the pile.

The static loading test was performed two weeks after the installation of the pile and the test schedule consisted of loading the pile in seven increments (the first increment was 1,585 kN) to a maximum load of 5,760 kN equal to the maximum jacked-in load, unloading and, then, re-loading the pile in nine increments. The maximum load in the re-loading, Incr. #8 of the static loading test, was 6,290 kN, 530 kN larger than the nominal maximum jacking load, at which load the pile plunged and the load applied could not be held but dropped to 6,050 kN.

Figure 17 shows the load-movement curves for the pile head, shaft, and toe, as well as the total pile shortening for the static loading test. The green lines are the load-movement curves produced in a simulation of the test, as will be discussed later. The re loading curve is parallel to the initial load-movement curve and the unloading curves. The figure suggests that the pile toe "failed" in a plunging mode after a toe penetration of about 5 mm. That the pile toe failed is a misinterpretation. Up to the final load in the first loading of the pile in the test (Incr.#7), the pile toe was in a re-loading mode, beyond Incr.#7 of the first loading, the pile response was in a virgin mode and, therefore, the movement was larger.

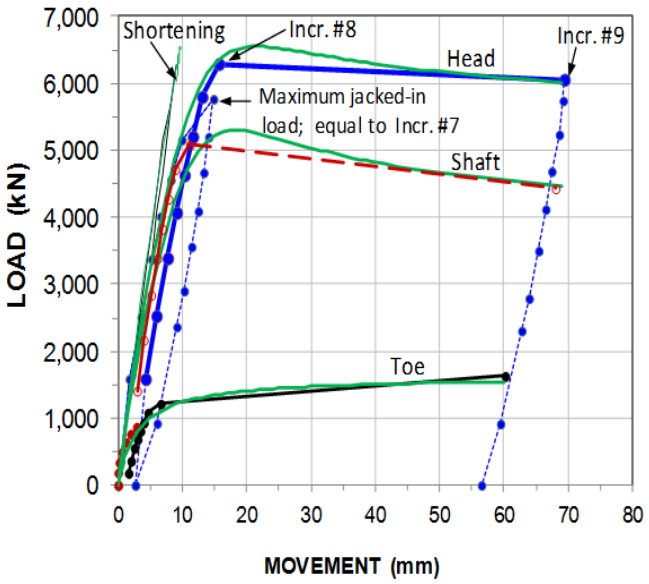


Figure 17 Static loading test load-movement curves for pile head, shaft, toe, and shortening

In preparation of the static loading test the pile was equipped with seven levels of Glostrext extensometers (Hanifah and Lee 2006), a extensometer-gage system based on anchors and measurements of pile shortening by means of vibrating wire technology. The test was performed two weeks after the installation.

Of course, considering the fact that the pile was installed by jacking, the static loading test was very similar to the jacking-procedure installation of the pile. Even the first loading of the test was really a re-loading of the pile. However, once the applied load went beyond the previous maximum loads, the loads were no longer re-loads and the stresses imposed are beyond previous stress levels, which is why much larger movement then resulted.

A jacked-in installation method leaves the pile with a maximum residual load. The measured load distribution is shown in Figure 18. On the assumption that the jacking left the pile with fully mobilized residual load (probably close to the fact), the distributions of true resistance and residual load are as shown in the figure. The residual load is due to fully mobilized negative skin friction down to 12.4 m depth below which a transfer to positive shaft resistance started. The force equilibrium was at a depth of 14.1 m, very close to the pile toe. A UniPile simulation of the true distribution established the beta-coefficients listed to the right of the figure. Naturally, the distributions of the true and residual loads depend on the assumption of fully mobilized residual load and there is no way of knowing to what extent the assumption is correct.

Had the jacked-in pile been supplied with a bidirectional cell assembly, the cell load would have included the residual load and been a "true" load. Indeed, if we assume that instead of the head-down test, a bidirectional cell had placed at the 14.1-m force equilibrium depth, then, under the assumption of fully mobilized residual load and that the bidirectional test would have been terminated at the very same load that was simulated for the gage level, the first four gage depths below the ground surface would not have reacted to the tests—they would have shown zero imposed load. (Which, most probably, would have given rise to some unease for the people monitoring the gages). The fifth and sixth gage depths would have indicated some small strain and the seventh gage below the cell assembly level would have measured much the same loads as were measured in the head-down test. The two dashed curves in the figure represent the distribution of the bidirectional cell test and the distribution that the strain-gage instrumentation would have indicated for the bidirectional test. As the pile is relatively short, the buoyancy and pore pressure effect would have been minimal.

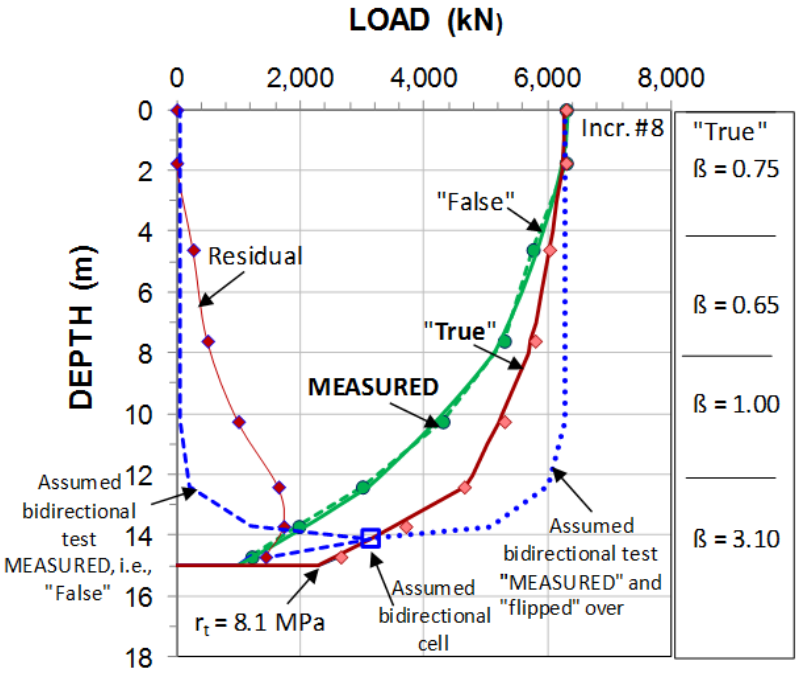


Figure 18 Distributions of "False,", "True", and Residual Loads with back-calculated ß-coefficients. The dashed curves show the "False" and "Flipped Over" distributions for an assumed bidirectional test.

The test on the jacked-in pile demonstrates the considerable effect residual loads can have on the results of a static loading test, and, that, in contrast to the conventional head-down test, a bidirectional test will provide the means for determining the true load and resistance distribution.

The question of presence and distribution of residual load affecting the results of a head-down test on an instrumented pile can be resolved by performing a tension test ("head-up" test) after the head-down test. As suggested in Figure 18, the "false" load distributions will plot on opposite sides of the "true" distribution.

## 3. INSTRUMENTATION

Regardless of the static loading test method used, for long piles and in a layered soil profile, it is necessary to provide the pile with instrumentation for monitoring the distribution of resistance along the pile. The instrumentation used is mostly vibrating-wire strain-gages. In bored piles, sometimes, extensometers are also used that determine the strain between two depths in the pile and, thus, average the influence due to necking and bulging. In a sense, extensometers are modern version of telltales, which are the system of instrumentation of old, but these days only used for direct measurements of, say, pile toe movement.

Determining load from strain measurements means multiplying the strain with the pile stiffness, EA, the modulus, E, and the cross sectional area, A. For a bored pile, the area is often different to the nominal area of the pile. Moreover, the modulus is a highly variable parameter (other than for steel piles). Not only is it different from concrete mix to concrete mix, the relation to measurable quantities such as strength is approximate at best. Even the modulus measured on samples made from the specific concrete batch (cubes or cylinders) and stored in ways similar to the concrete cast in the ground will not necessarily be the same as that of the pile (Fellenius 1989; 2014a, Amir et al. 2014). Then, it needs to be recognized that the modulus of concrete is not a constant, but reduces significantly with strain.

If the test is carried out to produce significant strain in the pile, that is, imposing strain larger than about 400 με, then, the modulus can be determined directly from the strain-gage records by means of the method of "incremental-stiffness", also called the tangent-modulus method as detailed by Fellenius (1989; 2014a). This method determines the stiffness, EA, of the pile, therefore, it eliminates or moderates the deliberation effort for determining the pile cross section. A further requirement is that the unit shaft resistance (the t-z relation) is neither particularly strain-hardening nor strain-softening.

The loads determined from strain-gage measurements are those imposed by the applied test loads. Any residual strains. i.e., loads, present in the pile before the start of the test, are extra and must be determined, or the true load and resistance distribution will not be known. Taking "zero" readings before installing the gages down the pile (and during the time before the start of the loading test), will help, but those records are affected by several conditions and actions unrelated to the soil set-up, such as strains built-in during concrete hydration, swelling of concrete from absorbing water from the soil (Fellenius et al. 2009, Kim et al. 2011). Driven steel piles are not immune to the problem, because they have locked-in strain from the uneven cooling after manufacturing and some of these strains can be released in the driving.

Residual load are usually considered caused by reconsolidation of the soil around the pile after installation/construction of the pile. Bored piles, as opposed to driven piles, normally show smaller such effect, but they are not always free from residual load. And, residual load can be induced by a prior test event, as evidenced by the preceding CFA case history.

One of the largest adverse effects on the evaluation of load from measured strain derives from unloading and reloading cycles included in the test. Such procedures are common. However, I have yet to see any such procedure produce any information that can add to the understanding of the pile and soil response to the test let alone a case where a such procedure would be helpful for a subsequent piled foundation design. The main effect of an

unloading/reloading is that the pile capacity becomes undefined and the instrumentation costs and efforts has been wasted.

It is important that a static loading test be performed using load increments of equal magnitude and that the duration of each load-holding be maintained the same throughout the entire test. Changing the increment magnitude or increasing or shortening the load-hold duration at any one load level will severely impair the evaluation of the strain-gage data. The load-holding duration can be short or long, but it must be the same throughout the test. Wherever provisions of different increment magnitudes, load-holding durations, or unloading/reloading cycles are included in guidelines or standards, in my strong opinion, weeding them out will be a real service to the profession.

For piles longer than the relatively short piles reported in the four case histories, to separate the shaft and toe resistances in a head-down test, instrumentation would be necessary with the difficulties of interpretation this entails. While a bidirectional test provides the true load, the analysis of test piles longer than 20 m will normally benefit from strain-gage instrumentation also for bidirectional tests.

If the strain-gage instrumentation indicates presence of residual load affecting the load distribution in a bidirectional test and the veracity of the evaluation of the gages is uncertain, then, comparing the gage records of the bidirectional test with those obtained in a head-down compression test with the cell draining (open) performed immediately after the bidirectional test will clearly indicate whether or not residual loads are present and how large they are.

## 4. CONCLUSIONS

The four case histories have illustrated the following main points.

1. As the shaft resistance for the individual pile elements is rarely ideally elastic-plastic, the pile capacity determined as the sum of the maximum shaft resistance of a series of pile elements is not the capacity one would interpret from the pile head load-movement curve.

2. Analysis of the results of a static loading test involving only measuring of the load and movement at the pile head will not be able to separate the shaft and toe resistances responses to the test loads. This difficulty can be avoided by performing a bidirectional test instead of the conventional head-down test.

3. The bidirectional test is often considered to be a replacement for conventional head-down test to twice the desired working load disregarding the fact that that it is a test method offering much more information and possibility for establishing the pile response than the conventional test can provide.

4. To establish the full response of a pile to load in a bidirectional test, it is recommend to place the cell assembly two or three pile diameters above the pile toe to ensure that the downward response is well determined. Then, if the resistance of the length above the cell assembly is not fully mobilized, it is easy and inexpensive to perform a tension test ("pull" test) on the length above the cell level, which will establish also the full response of the length above the cell assembly.

5. By fitting the results of a bidirectional test to an effective stress analysis and converting the fitted condition to an equivalent head-down load-distribution curve, or an equivalent head-down load-movement diagram, the full response of the pile is established.

6. The analysis of the dynamic tests on the CFA pile showed good agreement with the subsequent static loading test when taking into consideration that the dynamic test left the pile with some locked-in load (residual load), and increased the stiffness response of the pile. Back-analysis of the static test

established the virgin conditions for the pile. The simulated virgin load-movement curves for pile head, pile shaft, and pile toe agreed well with the CAPWAP results for the first dynamic test blow, which was given to the pile under virgin conditions.

7. For comparison of capacity between the results of a dynamic and a static test, the capacity of the static test should be according to the offset limit method. This not withstanding that when evaluating the results of the static loading test for other purposes, the individual may well pursue a capacity definition other than the offset limit. Doing that in the comparison dynamic to static, however, is not an apple-to-apple comparison.

8. The load by a bidirectional cell assembly at the cell location in the pile is unaffected by residual load (locked-in load) in the pile, i.e., the cell-measured load includes the residual load in the pile.

9. By providing the test piles with strain-gage instrumentation, the load distribution can be estimated and the toe resistance determined for the loads applied. However, instrumentation is sometimes difficult to evaluate correctly. Even when gages function properly and the pile cross sectional area is constant (as for the precast piles), the effect of strain-hardening and strain-softening can still result in significant uncertainty about the load distribution. Moreover, if residual loads are present in the pile at the test occasion, they will affect the loads determined from strain-gage instrumentation. An extrapolation of the test results to select longer or short piles could then be very much in error.

10. The presence of residual load particularly influences the load distribution determined in an instrumented pile tested in a head-down test, giving an exaggerated value of the shaft shear along the upper portion of the pile and a smaller than actual shaft shear along the lower portion. The toe resistance can appear very much smaller than actual. For a bidirectional test, the effect is the opposite above the cell assembly. However, as the bidirectional cell determines the true load, no instrumentation is necessary for short piles. It may be used for long piles, where then the bidirectional cell measurements would serve to calibrate the analysis for the residual load distribution.

11. If the strain-gage instrumentation indicates presence of residual load and the veracity of the evaluation is uncertain, performing a tension test (pull or uplift test) immediately after the head-down compression test will clearly indicate whether or not residual loads are present and how large they are. In a bidirectional test, the second test would be a head-down compression test with the cell draining (open).

## ACKNOWLEDGEMENTS

I am much indebted to my friend and colleague, Dr., Mauricio Ochoa for his critical review and constructive comments on the manuscript. I am also grateful for the comments and information offered by Messrs. Sergio C. Paraiso and Paulo Abreu.

## REFERENCES

Aoki, N. ,2000. Improving the reliability of pile bearing capacity prediction by the dynamic increasing energy test, DIET. Keynote Lecture, Proc. of the Sixth Int. Conference on the Application of Stress-Wave Theory to Piles. Sao Paolo, September 11-13, Balkema, pp. 635-650.

Amir, J.M., Amir, E.J., and Lam, C., 2014. Modulus of elasticity in deep bored piles. Proceedings of the DFI-EFFC International Conference on Piling and Deep Foundations, Stockholm, May 21-23, pp. 397-402.

Arcos Egenharia, 2014. Results of bidirectional test on two CFA piles in Sao Paolo, Brazil. Personal communication.

Davisson, M. T., 1972. High capacity piles. Proceedings of Lecture Series on Innovations in Foundation Construction, ASCE Illinois Section, Chicago, March 22, pp. 81-112.

Elisio, P.C.A.F., 1983. Celula Expansiva Hidrodinamica – Uma nova maneira de executar provas de carga (Hydrodynamic expansive cell. A new way to perform loading tests). Independent publisher, Belo Horizonte, Minas Gerais State, Brazil, 106 p.

Elisio, P.C.A.F., 1986. Celula expansiva hidrodinamica; uma nova maneira de ecutar provas de carga (Hydrodynamic expansion cell; a new way of performing loading tests). Proc. of VIII Congresso Brasileiro de Mecânica dos Solos e Engenharia de Fundações, VIII COBRAMSEF, Porto Alegre, Brazil, October 12-16, 1986, Vol. 6, pp. 223-241.

Fellenius, B.H., 1989. Tangent modulus of piles determined from strain data. ASCE, Geot. Engng. Division, the 1989 Foundation Congress, F.H. Kulhawy, Editor, Vol. 1, pp. 500-510.

Fellenius, B.H., 2013a. Capacity and load-movement of a CFA pile: A prediction event. GeoInstitute Geo Congress San Diego, March 3-6, 2013, Foundation Engineering in the Face of Uncertainty, ASCE, Reston, VA, James L. Withiam, Kwok-Kwang Phoon, and Mohamad H. Hussein, eds., Geotechnical Special Publication, GSP 229, pp. 707-719.

Fellenius, B.H., 2013b. An Excel template cribsheet for use with UniPile and UniSettle. Report to UniSoft Ltd. (www.Fellenius.net).

Fellenius, B.H., 2014a. Basics of foundation design, a text book. Revised Electronic Edition, [www.Fellenius.net], 410 p.

Fellenius, B.H., 2014b. Response to load for four different bored piles. Proc. of the DFI-EFFC International Conference on Piling and Deep Foundations, Stockholm, May 21-23, pp. 99-120.

Fellenius, B.H., Kim, S.R., and Chung, S.G., 2009. Long-term monitoring of strain in instrumented piles. ASCE J. of Geotechnical and Geo-environmental Engineering, 135(11) 1583-1595.

Glostrext Technology, 2013. Report on results of static axial compression loading test on instrumented spun pile at Bishan Street, Singapore, Report No.: S-A2-013-CSCG-ULT1.

Goble, G. G., Rausche, F., and Likins, G.E., 1980. The analysis of pile driving—a state-of-the-art. Proceedings of the 1st International Seminar of the Application of Stress-wave Theory to Piles, Stockholm, Edited by H. Bredenberg, A. A. Balkema Publishers Rotterdam, pp. 131-161.

Gregersen, O.S., Aas, G., and DiBiagio, E., 1973. Load tests on friction piles in loose sand. Proceedings of the 8th International Conference on Soil Mechanics and Foundation Engineering, ICSMFE, Moscow, August 12-19, 1973, Vol. 2.1, Paper 3/17, pp. 109-117.

Goudreault, P.A. and Fellenius, B.H. 2013. UniPile Version 5, Users and Examples Manual. UniSoft Ltd. [www.UniSoftLtd.com]. 99 p.

Hanifah, A.A. and Lee S.K., 2006. Application of global strain extensometer (Glostrext) method for instrumented bored piles in Malaysia. Proc. of the DFI-EFFC 10th Int. Conf. on Piling and Deep Foundations, May 31-June 2, Amsterdam.

Hunter A.H. and Davisson M.T., 1969. Measurements of pile load transfer. Proceedings of Symp. on Performance of Deep Foundations, San Francisco, June 1968, American Society for Testing and Materials, ASTM, Special Technical Publication, STP 444, pp. 106-117.

Kim, S.R., Chung, S.G., and Fellenius, B.H., 2011. Distribution of residual load and true shaft resistance for a driven instrumented test pile. Canadian Geotechnical Journal, 48(4) 384-398.

Meyerhof, G.G., Brown, J.D., and Mouland, G.D., 1981. Predictions of friction capacity in a till. Proceedings of the ICSMFE, Stockholm, June 15-19, Vol. 2, pp. 777-780.

Nordlund, R.L., 1963. Bearing capacity of piles in cohesionless soils. ASCE Journal of Soil Mech. and Foundation Engineering 89(SM3) 1-35.

Osterberg, J., 1989. New device for load testing driven piles and bored piles separating friction and end-bearing. Deep Foundations Institute, Proc. of the International Conf. on Piling and Deep Foundations, London, London June 2-4, Eds. J.B. Burland and J.M. Mitchell, A.A. Balkema, Vol. 1, pp. 421-427.

Osterberg, J.O., 1998. The Osterberg load test method for drilled shaft and driven piles. The first ten years. Deep Foundation Institute, Seventh International Conference and Exhibition on Piling and Deep Foundations, Vienna, Austria, June 15-17, 1998, 17 p.

Oliveira, M.A., Falconi, F.F., and Perez, W., 2008. Estaca hélice contínua – ensaio dinâmico e prova de carga estática. 6th Seminário de Engenharia de Fundações Especiais e Geotecnia, SEFE VI, Sao Paolo, Brazil, November 3-5, Vol. 1 pp. 423-431.

Rausche, F., Goble, G.G., and Likins, G.E., 1985. Dynamic determination of pile capacity. ASCE Journal of the Geotechnical Engineering Division 111(GT3) 367-383.

# APPENDIX

## FUNCTIONS FOR t-z AND q-z RESPONSES

The UniPile software (Goudreault and Fellenius 2013) includes the following five t-z and q-z functions for simulation of the pile load-movement response. Each soil layer can be assigned a different function. The various options are detailed by Fellenius (2014a).

The **Ratio Function**, a strain-hardening response independent of any ultimate load.

$$Q_n = Q_S \left( \frac{\delta_n}{\delta_S} \right)^{\theta} \qquad \text{(A1)}$$

where
$Q_n$ = any applied load
$\delta_n$ = movement for $Q_n$
$Q_s$ = any other applied load
$\delta_s$ = movement for $Q_S$
$\Theta$ = exponent

The Ratio Function means that for a doubling of load from, say, $Q_1$ to $Q_2$, and for Θ-exponents ranging from 0.2 through 0.9, the movement $\delta_2$ for $Q_2$ will increase by the following number of times the movement, $\delta_1$, for $Q_1$:

| Θ = | 0.2 | 0.3 | 0.4 | 0.5 | 0.6 | 0.7 | 0.8 | 0.9 |
|---|---|---|---|---|---|---|---|---|
| $\delta_2$ = | 32 | 10 | 6 | 4 | 3.2 | 2.7 | 2.4 | 2.2 |

The **Hyperbolic Function** (Chin-Kondner), a strain-hardening response.

$$Q_n = \frac{\delta_n}{C_1 \delta_n + C_2} \qquad \text{(A2)}$$

$$Q_\infty = \frac{1}{C_1} \qquad \text{(A3)}$$

$$C_2 = \delta_n \left( \frac{1}{Q_n} - C_1 \right) = \delta_n \left( \frac{1}{Q_n} - \frac{1}{Q_\infty} \right) \qquad \text{(A4)}$$

Where
$Q_n$ = any applied load
$Q_u$ = load at infinite movement
$\delta_n$ = movement for $Q_n$
$C_1$ = slope of the straight line in the $\delta/Q$ versus $\delta_n$ diagram
$C_2$ = y-intercept of the straight line in the $\delta/Q$ versus $\delta_n$ diagram
$Q_\infty$ = resistance at infinite movement

The $Q_u$ refers to the ultimate resistance at infinite movement. However, the ultimate is usually referred to as 100 % of the value mobilized at a finite movement, e.g., a common value is 5 mm for unit shaft resistance along a pile element. At whatever finite 100 % movement assumed, the inverse of the coefficient $C_1$ indicates the ratio (%) of load to the 100 % of the resistance at infinite movement.

The **Exponential Function** (van der Veen), essentially a plastic response.

$$Q_n = Q_S (1 - e^{-b\delta_n}) \qquad \text{(A5)}$$

Where
$Q_n$ = any applied load
$\delta_n$ = movement for $Q_n$
$Q_s$ = any other applied load
$b$ = an exponent

The benefit of the Van Der Veen's function is that the kink between the elastic and plastic lines is smoothened over.

The **Hansen Function**, a strain-softening response.

$$Q_n = \frac{\sqrt{\delta_n}}{C_1 \delta_n + C_2} \qquad \text{(A6)}$$

$$Q_u = \frac{1}{2\sqrt{C_1 C_2}} \qquad \text{(A7)}$$

$$\delta_u = \frac{C_2}{C_1} \qquad \text{(A8)}$$

Where $Q_n$ = any applied load

$Q_u$ = ultimate load
$\delta_n$ = movement for $Q_n$
$\delta_u$ = movement for $Q_u$
$C_1$ = slope of the load-movement curve plotted as $\sqrt{\delta_n}/Q_n$ versus $Q_n$
$C_2$ = y-intercept of the $\sqrt{\delta_n}/Q_n$ versus $Q_n$

The **Zhang Function**, a strain-softening response.

$$Q_n = \frac{\delta_n(a + c\delta_n)}{(a + b\delta_n)^2} \qquad \text{(A9)}$$

$$Q_n = \frac{1}{4(b - c)} \qquad \text{(A10)}$$

$$\Gamma = \frac{c}{Q_n b^2} \qquad \text{(A11)}$$

Where $Q_n$ = any applied load
$\delta_n$ = movement for $Q_n$
$a$ = constant
$b$ and $c$ = constants or factors that depend on a, $Q_n$, and $\delta_n$
$\Gamma$ = resistance at infinite movement (must be >0)

Once the value of "*a*" is decided on, then, "b" and "c" are determined by Eqs. A12 and A13, respectively, and, then, $\Gamma$ is determined by Eq. A11.

$$b = \frac{1}{2Q_n} - \frac{a}{\delta_n} \qquad \text{(A12)}$$

$$c = \frac{1}{4Q_n} - \frac{a}{\delta_n} \qquad \text{(A13)}$$

## USING THE FUNCTIONS

All five functions mentioned above are available for use in UniPile. Each "t-z/q-z" option shows an input screen and a graph of the force (%) and movement (mm or inch) and each is are correlated to the chosen inputs of soil layer resistance. The 100-% value of the force ("$r_u$") is the "ultimate" and the "$\delta_u$" is the movement for that force. (The $r_u$ and $\delta_u$ shown on the screen should rightly be denoted $r_{100}$ and $\delta_{100}$, because, they do not stand for the "ultimate", but indicate the resistance for the various soil elements within a soil layers and the movement for that resistance. In the five formulae, they are referred to as $Q_n$ and $\delta_n$).

All functions require input of the maximum movement value to show in the function graph and all functions, but the exponential, require input of the movement, $\delta_u$, for which the soil layer resistance (100 %-value) occurs. Thus, all curves will pass through the 100%/"$\delta_u$" point. The additional input to choose for the various functions determines the shape of the curve on both sides of the point.

### Ratio Function

The additional input for the Ratio Function is the value of the exponent, which, theoretically goes from 0 through unity. Usual ranges are 0.1 through 0.5 for shaft resistance and 0.4 through 0.8 for toe resistance. An exponent equal to 1.0 represents a straight line—elastic soil response. When using the function to fit, say, an actually observed pile-toe load-movement curve, the User will first have to input a toe resistance (soil layer input screen) that produces a calculated toe resistance equal to 100 % of that measured at a certain toe movement $\delta_u$, whichever movement the User now prefers to input as the 100-% movement. The User then activates "Analyze", selects the "Head-down loading-test simulation" for view. The display of the calculation results will be used to verify agreement between the measured and calculated values of load and movement. However, there will at first be little or no agreement between the measured and calculated load-movement curves. The user now adjusts the exponent and repeats action until the measured and calculated curves agree. It may well be that no exponent will provide full agreement. If so, the User selects another t-z/q-z function for fitting.

If, when fitting a Ratio Function q-z analysis made for, say, a 1,000-kPa toe n at, say, 30-mm

movement, and it is preferred to do the fit for either the toe resistance at, say, 12.5 mm movement or the movement for, say, a toe resistance of 500 kPa, Eq. A1 provides the particular fourth input parameter. Provided that the Θ-exponent is kept the same, the simulated load-movement curves will be the same for either of the three q-z inputs.

**Hyperbolic Function** (Chin-Kondner)

Similar to the other functions, applying the Hyperbolic Function starts by entering a movement value to represent the soil layer input of resistance, the 100-% value. The input of the "Slope, $C_1$" governs the shape of the curve. A $C_1$-value of 0.100 represents a constant 100-% resistance, which is not a meaningful input—the $C_1$-value must always be smaller. For example, a 65-mm toe movement for the 100-% input resistance and a $C_1$-value of 0.0098 will result in a q-z curve that reaches about 80 % at a toe movement of 5 mm. In contrast, a movement input of 10 mm together with a $C_1$-value of 0.0075 will also result in a q-z curve that reaches about 80 % at a toe movement of 5 mm, but the load at 65 mm will be 127 %. The former is almost "elastic-plastic" response, while the latter is a strain-hardening response.

**Exponential Function**

As mentioned, the Exponential Function applies to shaft resistance modeling and to cases where the response is almost elastic-plastic. The rise of the curve is at first almost vertical until close to the 100-% value where the curve changes to a horizontal (plastic) line. The exponent governs the curvature and the distance before the horizontal line. Using and adjusting the Hyperbolic Function to fit often produces the results faster.

**Hansen Function**

Similar to the exponential function, the Hansen Function is almost exclusively used for shaft resistance response. The shape of function curve is controlled by the movement and the $C_1$-inputs (note, the C1 of the Hansen function is defined somewhat similarly but still differently to that of the Ratio Function). In fitting calculations to actual measured values, the User decides which movement occurred when the ultimate soil resistance occurred, i.e., the peak value and the shape of the curve before and after this value. Note, however, that the movement and $C_1$ are interrelated. Change one and the other changes too. The $C_1$-value is only applied when the measured curve has been analyzed and fitted to a Hansen function separately (Fellenius 2013b), which results in a $C_1$-value for use as input instead of the movement value.

For the Hansen function, regardless of the input of $\delta_u$, $Q_u$, and $C_1$, the movement for the 80-% of $Q_u$ is always 0.25 of the $\delta_u$, movement.

**Zhang Function**

The Zhang Function, is a strain-softening response that produces a t-z curve very similar to the Hansen curve. As for the other functions, the movement for which the peak resistance (100 %) is observed is input first. The coefficient "a" is then used to adjust the shape of the curve to fit.